Published by Avanti Publishers

Journal of Chemical Engineering Research Updates

ISSN (online): 2409-983X

Pectin-based Bioink and Bioprinting Parameter Optimization and Industrialization

Alexis Berka[#], Aidan Callahan[#], Sonia Grade[#], Benjamin Lilienkamp[#], Annika Peters[#], Rebecca Salzman[#], Mason Dopirak and Wujie Zhang[*]

Chemical and Biomolecular Engineering Program, Department of Physics and Chemistry, Milwaukee School of Engineering, Milwaukee, WI 53202, USA

ARTICLE INFO

Article Type: Research Article

Academic Editor: Zhijie Chen

Keywords:
Industrial scale-up
Bioink formulation
Parameter optimization
Extrusion-based bioprinting
Tissue engineering applications

Timeline:
Received: June 18, 2025
Accepted: July 22, 2025
Published: August 06, 2025

Citation: Berka A, Callahan A, Grade S, Lilienkamp B, Peters A, Salzman R, Dopirak M, Zhang W. Pectin-based bioink and bioprinting parameter optimization and industrialization. J Chem Eng Res Updates. 2025; 12: 50-57.

DOI: https://doi.org/10.15377/2409-983X.2025.12.3

ABSTRACT

Bioprinting for tissue engineering and regenerative medicine offers a promising solution to the growing demand for organ transplants. A pectin-based bioink was engineered to offer cost-effectiveness and operational simplicity. This project focuses on the commercialization and industrial production of this bioink. The bioink formulation and bioprinting parameters for extrusion-based bioprinting were optimized, as extrusion-based bioprinters are most commonly used in bioprinting. The optimization process focused on structural integrity, resolution, and cell viability. Additionally, an industrial-scale production process was designed using SuperPro Designer. The bioink formulation with optimized bioprinting parameters shows great potential for extrusion-based bioprinting with scalable manufacturing capabilities.

[#]Equal contribution

*Corresponding Author
Email: zhang@msoe.edu
Tel: +(1) 414-277-7438

©2025 Berka *et al*. Published by Avanti Publishers. This is an open access article licensed under the terms of the Creative Commons Attribution Non-Commercial License which permits unrestricted, non-commercial use, distribution and reproduction in any medium, provided the work is properly cited. (http://creativecommons.org/licenses/by-nc/4.0/)

1. Introduction

Every day in America, 13 individuals on the transplant waitlist die due to the lack of life-saving donated organs/tissues. With a new person being added to the transplant waitlist every 8 minutes, the list is growing exponentially with no effective solutions (Fig. **1**) [1]. Bioprinting offers an alternative approach to this issue. Bioinks can be derived from many sources, either natural or synthetic, with each having unique properties for a diverse range of applications [2]. Natural biopolymers are biocompatible, biodegradable, and mimic the native tissue environment which gives rise to advantageous cellular responses [3, 4]. Synthetic biopolymers are desirable because of their modifiable features such as molecular weight and structure [4].

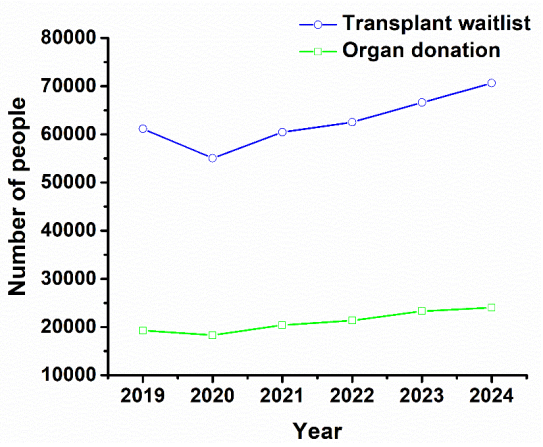

Figure 1: Transplant waitlist compared to organ donation statistics.

Different bioprinting methods have been utilized in the fabrication of complex solid organs including the heart, liver, kidney, and spleen [5]. These methods lead to improvements in personalized medical therapies by fabricating patient-specific prints [6]. Extrusion is one of the most common mechanisms for bioprinting due to its simplicity, affordability, and scalability [7]. The bioprinting process enables the fabrication of functional 3D structures using various bioinks extruded through pneumatic or mechanical printers. Pneumatic methods utilize compressed air for extrusion processes [8]. The printing pressure must be optimized to generate stable, uniform, and continuous filaments [8]. High pressures lead to unstable flow and low pressures cause irregularities in the print. Printing parameters affecting the pressure range include nozzle design, bioink viscosity, and yield stress [8]. Mechanical methods include piston and screw-driven processes. Piston-driven bioprinting allows for direct control of extrusion through the nozzle, whereas screw-driven configurations are preferred for bioinks with higher viscosity [9]. Pneumatic printers have simpler components making them user-friendly, but the prints have lower quality due to lack of controlling precision [10]. Mechanical printers are more complex to use and may lead to improvements in shape fidelity [10].

A pectin-based bioink has been developed. The two major components that ensure structural stability of the bioink are pectin and Pluronic F-127 [11-13]. Pectin is a natural linear polysaccharide consisting of α-1-4 linked D-galacturonic acid residues [14] that forms a stable hydrogel in the presence of a divalent cation such as Ca^{2+} [11]. This arises from the coordination interactions between the electron-rich hydroxyl and carboxyl groups of pectin and the divalent cation [15]. Pectin-based hydrogels have shown great potential for various biomedical applications such as drug delivery and tissue engineering [15, 16]. Pluronic F-127 is a copolymer of polyethylene oxide and polypropylene oxide. It is used to maintain the initial integrity of the print before the divalent cation is added. Pluronic F-127's mechanical properties stem from its unique ability to change from a liquid to a gel at 37 °C. Then, pectin is gelled with a divalent cation to form the permanent structure [11-13]. This novel approach is faster and requires only one syringe [11].

This project aims to realize the commercialization of a pectin-based bioink by optimizing its formulation and bioprinting parameters. Both pneumatic and mechanical extrusion-based bioprinting parameters were optimized. The industrial production process was designed using SuperPro Designer.

2. Materials and Methods

2.1. Materials

Pluronic F-127 and pectin were obtained from Sigma-Aldrich (St. Louis, MO) and WillPowder (Miami Beach, FL) respectively. D-Mannitol, N-2-hydroxyethylpiperazine-N-2-ethane sulfonic acid (HEPES), and $CaCl_2$ were obtained from Sigma-Aldrich (St. Louis, MO). A bioprinter (BIO X™, Cellink; Philadelphia, PA), including both pneumatic and syringe pump printheads, was used for bioprinting.

2.2. Bioink Preparation

The composition and function of each component are summarized in Table **1**. In brief, pectin and Pluronic F-127 are the major constituents of the bioink. Pluronic F-127 provides initial integrity during bioprinting due to gelation at a higher temperature, while pectin gives permanent structure due to crosslinking.

Table 1: Bioink components and their functions.

Component	Function
Pectin	Permanent structure
Pluronic F-127	Initial integrity and thermal sensitivity
D-Mannitol	Maintain osmolarity and antioxidative capabilities [23]

Different bioink formulations, T1-T3, were developed by varying the concentrations of pectin and Pluronic F-127. The base formulation consisted of 3.5 % (w/v) pectin, 20 % (w/v) Pluronic F-127, and 0.3 M mannitol. T1 contained an increased pectin concentration (5 %), T2 featured a higher Pluronic F-127 content (30 %), and T3 included elevated levels of both pectin (5 %) and Pluronic F-127 (30 %). Preliminary testing identified T1 and T3 as the only viable formulations. These modifications were designed to improve the structural integrity and printing resolution of the extruded constructs. Fig. (**2**) illustrates the bioink preparation process.

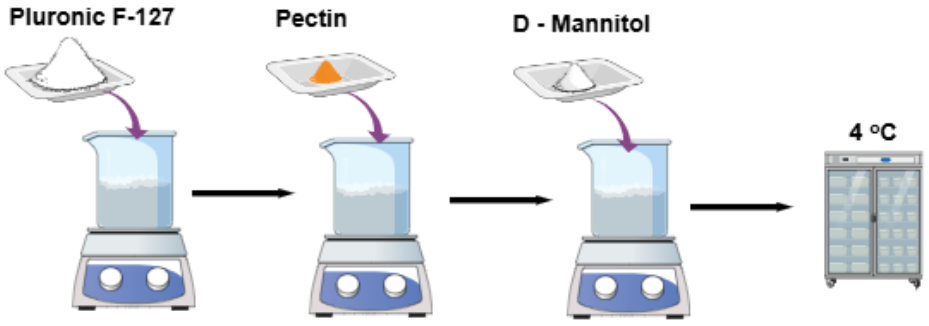

Figure 2: Schematic of the bioink preparation process.

2.3. Bioprinting Process

The testing range for each printing parameter was evaluated across non-printhead-specific settings, pneumatic printhead settings, and syringe pump printhead settings (Fig. **3**).

During bioprinting, bioink was first loaded into a 3-mL syringe and then the syringe was fixed to the printhead. Printing parameters, including printer bed temperature, were set. The bioink was extruded to the heated printer bed and the structural integrity was maintained initially due to the gelation of Pluronic F-127. Warm (~37 °C) 150 mM $CaCl_2$ was added around the scaffold to gel the pectin, forming permanent structure.

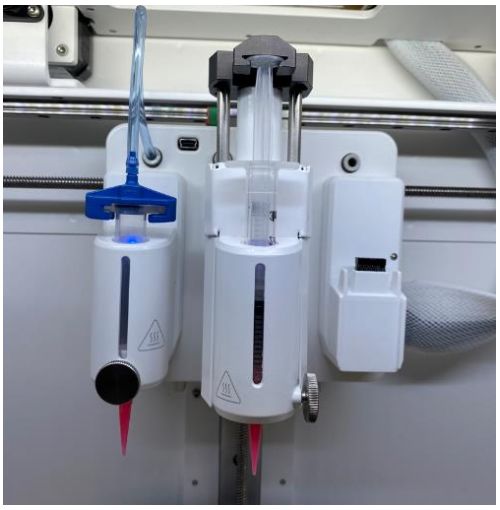

Figure 3: Image of the pneumatic (left) and syringe pump (middle) printheads of the Cellink BIO X™ printer.

2.4. Cell Culture and Cell Viability Assessment

MDA-MB-231 cells were cultured in Dulbecco's Modified Eagle Medium (DMEM; high glucose) and maintained in a humidified CO_2 incubator (5 %) at 37 ºC. The medium was supplemented with 10 % Fetal Bovine Serum, 100 U/mL penicillin, and 100 mg/L streptomycin. Cells were suspended in DPBS (50 µL) and then gently mixed with the bioink (containing HEPES with a final concentration of 10 mM) to reach a final cell density of 1×10^6 cells/mL. Bioprinting was performed under the optimized printing parameters. Cell viability was assessed using the LIVE/DEAD™ Viability/Cytotoxicity Kit for Mammalian Cells (L3224; ThermoFisher Scientific, Waltham, MA). Both Calcein-AM (for live cells) and ethidium homodimer-1 (for dead cells) were added to the medium with a final concentration of 5 µM each. After incubation for 5 min, the samples were assessed under a fluorescent microscope [16].

3. Results and Discussion

3.1. Bioink Formulation Optimization

The results of constructs printed using the base bioink formulation were found to be inconsistent; hence, various formulations were developed (T1-T3). T1 successfully produced high-resolution, reproducible structures across a range of bioprinting parameters. The optimal bioink temperature for T1 required it to be heated to 15 - 22 °C. However, the addition of $CaCl_2$ led to unstable layering as extrusion progressed due to the increased pectin concentration. T2 failed to produce a desirable construct. T3, which included increased concentrations of both pectin and Pluronic F-127, was observed to be the optimal formulation. It demonstrated promising short- and long-term gelation properties and resulted in high resolution and repeatable prints. Short-term gelation maintains the print structure eliminating the need for the addition of $CaCl_2$, which contributed to improved structural integrity and consistency. The optimal bioink temperature was 5 - 16 °C, allowing its use directly from refrigeration unlike T1. Based on the reliability and performance of T3, it was used for further studies.

3.2. Bioprinting Parameters Optimization

Optimal printing parameters are critical to ensure precise and reliable fabrication. Unoptimized conditions resulted in inconsistent prints, as shown in Fig. (**4**). To optimize the bioprinting parameters, evaluation was performed by printing a $10 \times 10 \times 5$ mm cuboidal structure consisting of 12 layers. Bioprinting process optimization was first conducted using a pneumatic printhead. The print bed was maintained at 40 °C to facilitate solidification of Pluronic F-127, forming the initial structure. The bioprinting parameters were optimized based on the established parameters for the base bioink: printing speed was set between 10–15 mm/s with a layer height of 1.2 mm. Additionally, printing pressure was set at 20 kPa, with a pre-flow rate of 0-5 mm/s and a post-flow rate of

5 mm/s. It was found that the pressure is bioink temperature-dependent (i.e., the lower bioink temperature, the lower required pressure). Then, syringe pump printhead optimization was performed. The printing parameters were found to be similar to those of the pneumatic printhead.

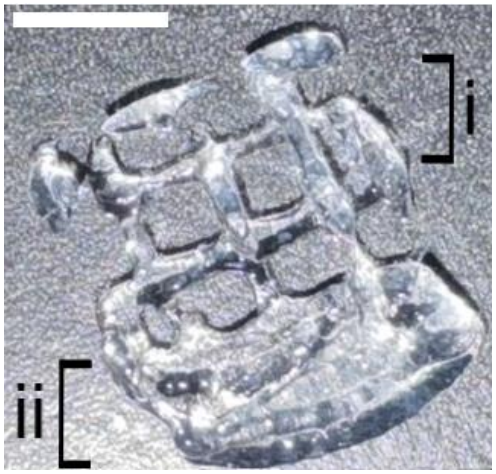

Figure 4: Image of incomplete structure (I) and low resolution (II) prints produced under non-optimized parameters. Scale bar represents 5 mm.

Optimized printing parameters are summarized in Table **2**. Furthermore, complex geometries were fabricated with the optimized parameters, such as an aortic valve (Fig. **5**).

Table 2: Operational and optimized bioprinting parameters.

	Non-Printhead Specific Settings				Pneumatic Printhead Specific Settings				Syringe Pump Printhead Specific Settings	
	Nozzle Size	**Bed Temp (°C)**	**Layer Height (mm)**	**Ink Temp (°C)**	**Pressure (kPa)**	**Pre Flow (ms)**	**Post Flow (ms)**	**Speed (mm/s)**	**Extrusion Rate (µL/s)**	**Speed (mm/s)**
Operational Range	15 - 20 gauge conical	35 - 50	0.41 - 1.5	4 - 28	10 - 60	-10 - 10	0 - 10	5 - 25	1 - 13	5 - 25
Optimized Range	16 - 18 gauge conical	40	0.41 - 0.45	5 - 16	30 - 55	-6	5	5	8	10

3.3. Industrial Production Process Design

The industrialization process was modeled using SuperPro Designer. A batch bioreactor was preferred as the vessel for bioink formulation due to its quality of mixing [17]. A cooling jacket and mechanical agitator were incorporated into the design as substitutes for the lab-scale ice bath and stir bar. Pluronic F-127 is first added in 1.5 g increments using a conveyor belt system to ensure uniform distribution. This is followed by the gradual addition of pectin, where continuous agitation facilitates complete dissolution of the components. D-mannitol is added last and aseptic conditions are maintained throughout the process to ensure sterility.

After mixing, the bioink proceeds through a fluid flow valve into the filling stage, where it is partitioned into 15 mL sterile vials. The bioink-filled vials are labeled and packaged for distribution to hospitals and bioprinting facilities. A critical aspect of the production process is the sterility of packaging [18]. The most used practice in industry is implementing a large-scale aseptic filling plant capable of completing tasks such as washing, sterilization, and closing of vials [19]. This is followed by external cleaning, labeling, and final packaging. These

processes provide a completely sterile and aseptic environment for the production and distribution of clinical-grade bioink (Fig. **6**).

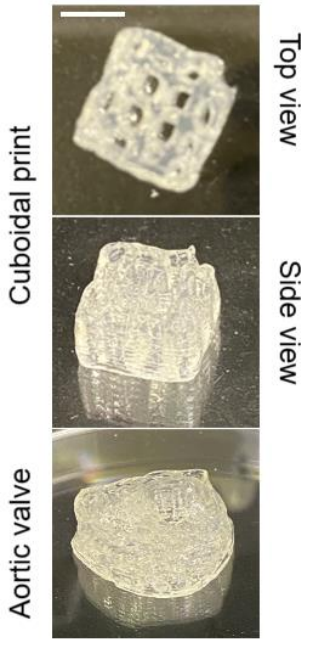

Figure 5: Image of constructs printed under optimized parameters using a pneumatic printhead. Scale bar represents 5 mm.

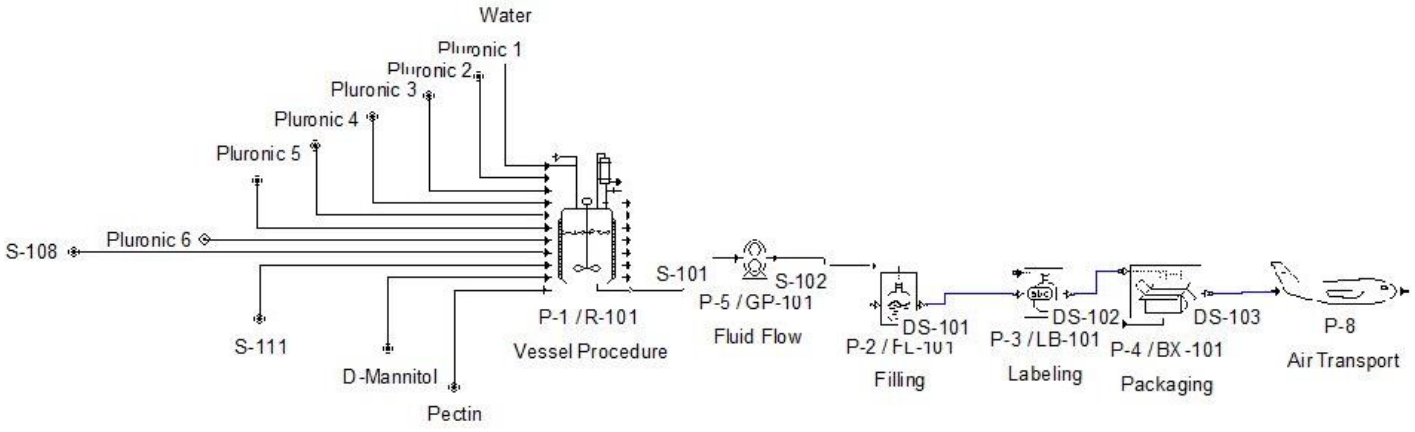

Figure 6: Designed process for the industrial bioink production.

3.4. Biocompatibility of the Bioink

The novel bioink containing MDA-MB-231 cells was loaded into a syringe, and bioprinting was carried out under the optimized parameters. Cell viability within the printed constructs was assessed using the LIVE/DEAD™ Viability/Cytotoxicity Kit. Calcein-AM, a cell-permeable dye, is converted to calcein and retained in live cells, producing intense green fluorescence. In contrast, ethidium homodimer-1 penetrates only cells with compromised membranes and binds to nucleic acids, resulting in bright red fluorescence [20]. Viability measurements taken immediately after bioprinting (day 0) and after three days of incubation (day 3) both indicated high cell survival rates, with approximately 99% viability, as shown in Fig. (**7**). These results demonstrate that the bioink is biocompatible and that the bioprinting process does not adversely impact cell viability. This challenges the traditional view that cell viability is typically lower following extrusion-based bioprinting compared to other printing methods, highlighting the benefit of this bioink [21, 22].

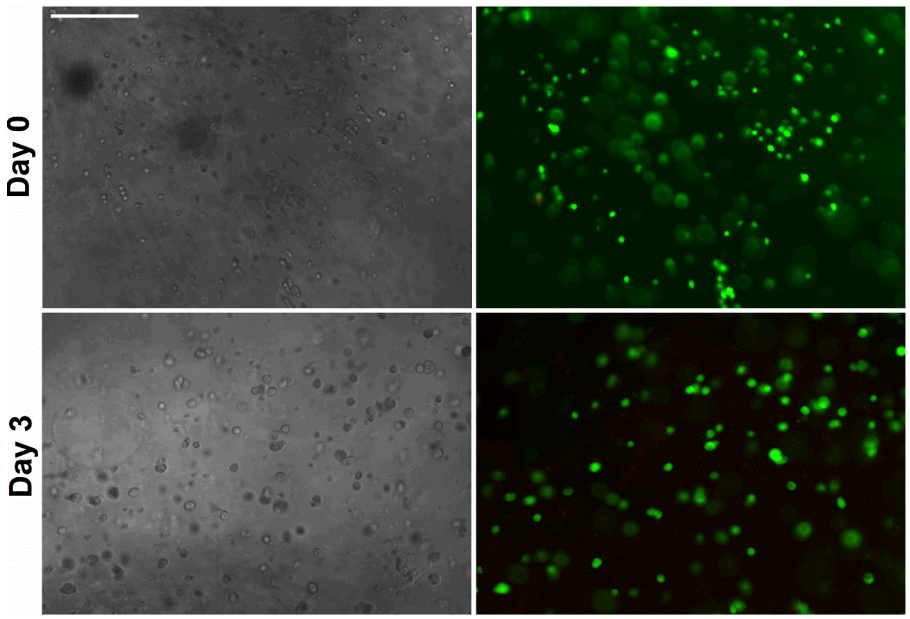

Figure 7: Microscopic images of cells within the printed scaffold. Left: bright field images, Right: merged fluorescent images. Scale bar represents 100 µm.

4. Conclusion

A pectin-based bioink formulation, along with its associated pneumatic and mechanical extrusion-based bioprinting parameters, was optimized. This dual optimization of both bioink composition and bioprinting conditions resulted in stable, high-fidelity constructs with a high cell viability of 99%. The industrialization process was modeled for scalable production using SuperPro Designer, ensuring the bioink can be efficiently manufactured and distributed. Future directions include cell behavior within the bioprinted scaffold, vascularization potential, and industrial production process optimization. Overall, there is immense potential for bioink in tissue engineering and regenerative medicine.

Conflict of Interest

The authors declare no conflict of interest.

Funding

This work was partially supported by the seed grant from the MSOE Innovent center.

Acknowledgments

The Authors would like to acknowledge De'Jorra Valentine for her technical assistance.

References

[1] Health Resources & Services Administration. Organ Donation Statistics. Available from: https://www.organdonor.gov/learn/organ-donation-statistics.

[2] Raees S, Ullah F, Javed F, Akil HM, Khan MJ, Safdar M, *et al*. Classification, processing, and applications of bioink and 3D bioprinting: A detailed review. Int J Biol Macromol. 2023; 232: 123476. https://doi.org/10.1016/j.ijbiomac.2023.123476

[3] Carrow JK, Kerativitayanan P, Jaiswal MK, Lokhande G, Gaharwar AK. Polymers for Bioprinting. In: Atala A, Yoo JJ, Eds. Essentials of 3D Biofabrication and Translation. Boston: Academic Press; 2015. p. 229-48. https://doi.org/10.1016/B978-0-12-800972-7.00013-X

[4] Reddy MSB, Ponnamma D, Choudhary R, Sadasivuni KK. A comparative review of natural and synthetic biopolymer composite scaffolds. Polymers (Basel). 2021; 13(7): 1105. https://doi.org/10.3390/polym13071105

[5] Wang X, Zhang D, Singh YP, Yeo M, Deng G, Lai J, *et al*. Progress in organ bioprinting for regenerative medicine. Engineering. 2024; 42: 121-42. https://doi.org/10.1016/j.eng.2024.04.023

[6] Shopova D, Yaneva A, Bakova D, Mihaylova A, Kasnakova P, Hristozova M, *et al*. (Bio)printing in personalized medicine—opportunities and potential benefits. Bioengineering. 2023; 10(3): 287. https://doi.org/10.3390/bioengineering10030287

[7] Boularaoui S, Al Hussein G, Khan KA, Christoforou N, Stefanini C. An overview of extrusion-based bioprinting with a focus on induced shear stress and its effect on cell viability. Bioprinting. 2020; 20: e00093. https://doi.org/10.1016/j.bprint.2020.e00093

[8] Ramesh S, Harrysson OLA, Rao PK, Tamayol A, Cormier DR, Zhang Y, *et al*. Extrusion bioprinting: Recent progress, challenges, and future opportunities. Bioprinting. 2021; 21: e00116. https://doi.org/10.1016/j.bprint.2020.e00116

[9] Ozbolat IT, Hospodiuk M. Current advances and future perspectives in extrusion-based bioprinting. Biomaterials. 2016; 76: 321-43. https://doi.org/10.1016/j.biomaterials.2015.10.076

[10] Zhang YS, Haghiashtiani G, Hübscher T, Kelly DJ, Lee JM, Lutolf M, *et al*. 3D extrusion bioprinting. Nat Rev Methods Primers. 2021; 1(1): 75. https://doi.org/10.1038/s43586-021-00078-3

[11] Banks A, Guo X, Chen J, Kumpaty S, Zhang W. Novel bioprinting method using a pectin-based bioink. Technol Health Care. 2017; 25(4): 651-5. https://doi.org/10.3233/THC-160764

[12] Johnson DL, Ziemba RM, Shebesta JH, Lipscomb JC, Wang Y, Wu Y, *et al*. Design of pectin-based bioink containing bioactive agent-loaded microspheres for bioprinting. Biomed Phys Eng Express. 2019; 5(6): 067004. https://doi.org/10.1088/2057-1976/ab4dbc

[13] Stealey S, Guo X, Ren L, Bryant E, Kaltchev M, Chen J, *et al*. Stability improvement and characterization of bioprinted pectin-based scaffold. J Appl Biomater Funct Mater. 2019; 17(1): 2280800018807108. https://doi.org/10.1177/2280800018807108

[14] Zieman J, Cohan M, Wang Y, De La Sancha A, Kanungo M, Azzouz R, *et al*. Development of gelatin-coated hydrogel microspheres for novel bioink design: A crosslinker study. Pharmaceutics. 2023; 15(1): 90. https://doi.org/10.3390/pharmaceutics15010090

[15] Chai A, Schmidt K, Brewster G, Peng Xiong L, Church B, Wahl T, *et al*. Design of pectin-based hydrogel microspheres for targeted pulmonary delivery. Gels. 2023; 9(9): 707. https://doi.org/10.3390/gels9090707

[16] Wu Y, Gu S, Cobb JM, Dunn GH, Muth TA, Simchick CJ, Li B, *et al*. E2-loaded microcapsules and bone marrow-derived mesenchymal stem cells with injectable scaffolds for endometrial regeneration application. Tissue Eng Part A. 2023; 30(3-4): 115-30. https://doi.org/10.1089/ten.tea.2023.0238

[17] Caccavale F, Iamarino M, Pierri F, Tufano V. Introduction. In: Control and Monitoring of Chemical Batch Reactors. London: Springer; 2011. p. 1-7. https://doi.org/10.1007/978-0-85729-195-0_1

[18] Adler M, Allmendinger A. Filling unit operation for biological drug products: Challenges and considerations. J Pharm Sci. 2024; 113(2): 332-44. https://doi.org/10.1016/j.xphs.2023.11.017

[19] Bhamra K, Harrison P, Phillips J, Hale G. Aseptic vial filling. In: George AJT, Urch CE, Eds. Diagnostic and Therapeutic Antibodies. Totowa, NJ: Humana Press; 2000. p. 313-7. https://doi.org/10.1385/1-59259-076-4:313

[20] Zhang W, Yang G, Zhang A, Xu LX, He X. Preferential vitrification of water in small alginate microcapsules significantly augments cell cryopreservation by vitrification. Biomed Microdevices. 2010; 12(1): 89-96. https://doi.org/10.1007/s10544-009-9363-z

[21] Murphy SV, Atala A. 3D bioprinting of tissues and organs. Nat Biotechnol. 2014; 32(8): 773-85. https://doi.org/10.1038/nbt.2958

[22] Knowlton S, Onal S, Yu CH, Zhao JJ, Tasoglu S. Bioprinting for cancer research. Trends Biotechnol. 2015; 33(9): 504-13. https://doi.org/10.1016/j.tibtech.2015.06.007

[23] Zhang W, Zhao S, Rao W, Snyder J, Choi JK, Wang J, *et al*. A novel core-shell microcapsule for encapsulation and 3D culture of embryonic stem cells. J Mater Chem B. 2013; 1(7): 1002-9. https://doi.org/10.1039/C2TB00058J